Chen, C., Lai, D., and Chen, Q. 2020. "Energy analysis of three ventilation systems for a large machining plant," *Energy and Buildings*, 224:110272.

Energy Analysis of Three Ventilation Systems for a Large Machining Plant

Chuanming Chen[1], Dayi Lai[2,*] and Qingyan Chen[3]

[1]School of Environmental Science and Engineering, Tianjin University, Tianjin 300072, China
[2]Department of Architecture, School of Design, Shanghai Jiao Tong University, Shanghai 200240, China
[3]School of Mechanical Engineering, Purdue University, West Lafayette, IN 47905, USA

[*]*Corresponding email: dayi_lai@sjtu.edu.cn*

Abstract
Manufacturing industries play an important role in economic development, but a large amount of energy is consumed in the removal of pollutants and heat generated on the manufacturing floor. An efficient ventilation system is needed for improving indoor air quality and thermal comfort at reduced energy cost. This study studied a displacement ventilation system with diffusers around columns for a machining plant, and compared its energy consumption with that of a perfect mixing ventilation system and the existing ventilation system in the plant. This investigation used computational fluid dynamics (CFD) to determine the vertical air temperature gradient in the plant, and the impact of temperature gradient on energy was estimated by means of building energy simulations (BES). The annual energy cost for the improved displacement ventilation system was 17.5% lower than that for mixing ventilation and 20.3% lower than for the existing ventilation system. However, because a large amount of outdoor air was used in winter, the heating energy consumption with the displacement ventilation was slightly higher than with the other two ventilation systems.

Keywords: Energy simulation; Indoor air quality; Thermal comfort; Displacement ventilation

1. Introduction

The China Energy Statistical Yearbook [1] reported that the manufacturing industry consumed 2.45 billion tons of standard coal equivalent energy in 2017, which accounted for 54.7% of the total national energy consumption. Because manufacturing processes generate large amounts of pollutants and heat [2], industrial buildings must use a lot of energy for air conditioning and ventilation to maintain a healthy and thermally comfortable environment [3]. A study of seven factories showed that air conditioning and ventilation systems accounted for up to 88.3% of the total building energy consumption for different types of industrial buildings [4]. In addition, most industrial buildings use mixing ventilation systems, and the ventilation efficiency of mixing ventilation system was low [5-9]. Therefore, an efficient ventilation system is required to ensure indoor air quality and thermal comfort at reduced energy cost.

The supply air outlets of mixing ventilation systems are often installed in the ceiling. It is difficult to supply air directly to the occupied zone, and energy is often wasted because of poor ventilation efficiency. Advanced ventilation systems could improve heat removal efficiency [10,11] and pollutant removal efficiency [12,13]. Compared with the traditional mixing ventilation system, displacement ventilation supplies fresh air directly at floor level in order to dilute contaminants. Cao et al. [14] reviewed the energy performance of various ventilation systems in office buildings and experimental chambers, and found that displacement ventilation provided a 20–34% reduction in energy use in comparison with mixing ventilation. Currently, very few studies have been conducted in industrial buildings to investigate the energy performance of different ventilation systems.

Caputo and Pelagagge [4] proposed a retrofit hybrid displacement ventilation system for an industrial building and found that its annual energy consumption was reduced by 50% compared with that of a mixing ventilation system. However, the annual result was deduced from field measurements performed within a single day. Such simplification may lead to large errors. In addition, field measurements are often time-consuming and costly. In contrast, building energy simulations (BES) can quickly provide detailed results at low cost [15]. For example, Lau and Chen [5] simulated the annual building energy consumption for a manufacturing workshop with floor-supply displacement ventilation in five climate regions in the United States. The authors concluded that displacement ventilation could save cooling energy in industrial buildings in most of the climate regions in the U.S. The simulation considered only thermal comfort and not indoor air quality. Since many industrial processes generate large amounts of pollutants, it is important to study the efficiency of contaminant removal by the ventilation system when performing energy simulations.

Most energy simulations assume uniform indoor air temperature [16]. However, in industrial buildings, vertical temperature stratification exists because of high ceilings [8]. In addition, pollutant removal efficiency has an impact on energy consumption. For the sake of accuracy, energy simulations should consider the indoor air distribution. The above simulation by Lau and Chen [5] and a study by Mateus and da Graça [17] both used three-node zonal models for the temperature stratification that is presented with a displacement ventilation system. However, the zonal models were based on simplified airflow patterns [18], and thus their applicability to industrial buildings was limited [19].

Unlike zonal models, computational fluid dynamics (CFD) can be applied in industrial plants to predict air temperature and pollutant stratifications [20]. Chen and van der Kooi [21] and Negrao [22] proposed the coupling of an energy simulation program with CFD in order to accurately calculate air temperature and pollutant distributions. Later, Zhai et al [23] analyzed different coupling strategies and concluded that stable and exclusive solutions do exist [24]. However, CFD requires intensive computational resources, and direct coupling of CFD with BES entails a long computing time [25]. The time needed for one hourly coupling simulation of a simple room was reported as 6.2 h [26]. Thus, it would be too expensive to simulate the annual (8760 h) energy consumption for a large factory. To reduce computing time, many studies have tried to couple CFD with BES indirectly [27-31] by using a fixed airflow pattern predicted by CFD in a building energy simulation. However, in actual situations, day-to-day airflow fields may vary greatly with the outdoor climate and air conditioning load, and large errors would emerge in energy prediction.

To balance accuracy and speed in simulating the annual energy consumption by a ventilation system in a large factory, this study proposed a framework for indirect coupling of CFD and BES by assuming that the air temperature gradient varied linearly with air conditioning load [21]. Under the same average air temperature and indoor air quality levels, this investigation studied annual energy consumption for a machining plant with different three ventilation systems: mixing ventilation, existing ventilation, and displacement ventilation.

2. Method

Figure 1 shows the research flow chart for this study. First, field measurements were performed in a machining plant to acquire essential information for energy simulations and validation. Based on the information about the building and ventilation system from on-site measurements, numerical simulation models were created in BES and CFD programs. The indoor air temperature and energy consumption obtained from field measurements were used to calibrate and validate the indirect coupling simulation. The validated models were then utilized to compare the energy consumption of mixing ventilation, existing ventilation, and displacement ventilation in this machining plant.

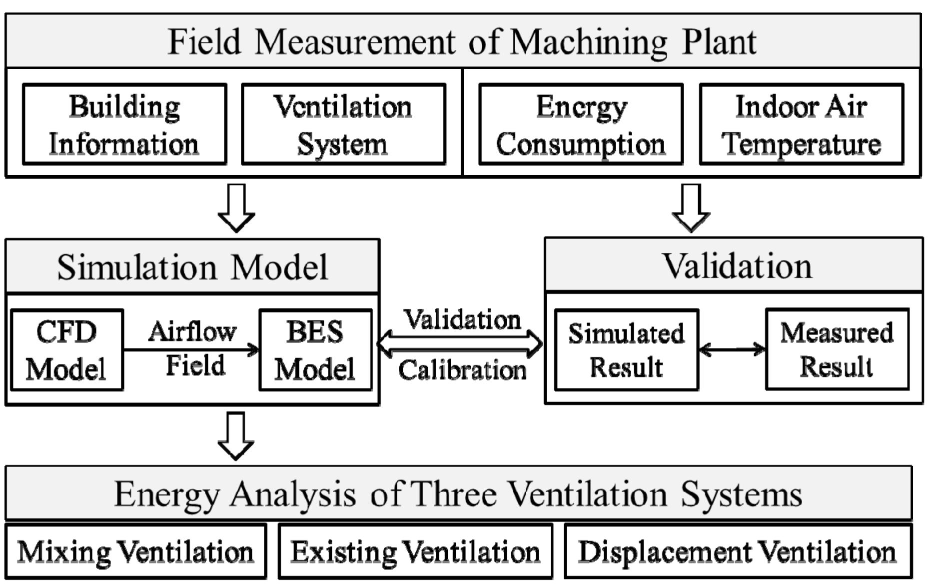

Figure 1. Research flow chart for present study

2.1 Machining plant studied

A machining plant in Tianjin, China, was selected for this study to compare energy consumption with different ventilation systems. The selected plant was a typical industrial building with a high ceiling, complex air conditioning system, and intense generation of heat and pollutants. The single-story building had a floor area of 27,540 m^2 (306 m$\times$90 m) and ceiling height of 8 m. Figure 2 shows the layout of the machining plant, which housed many production lines consisted of two rows of machining equipment that distributed throughout the building and several furnaces that located in heat treatment zone. Temperature sensors were installed in the plant to control HVAC system. Both of manufacturing processes would generate heat and pollutants. Therefore, a large amount of energy would be consumed by the HVAC system in the plant for indoor air quality and thermal comfort.

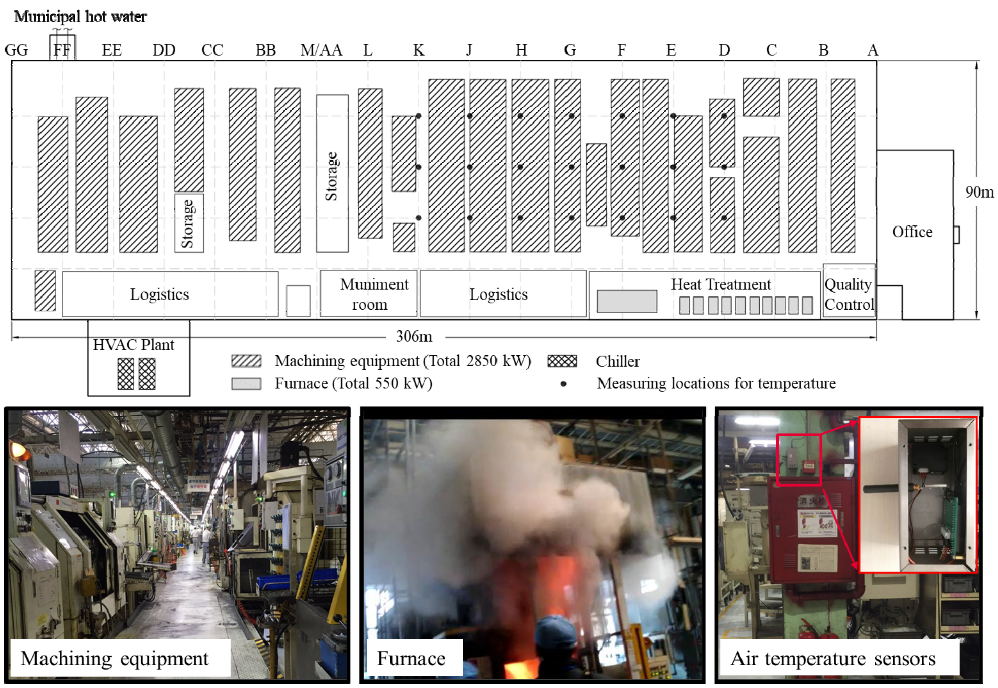

Figure 2. Layout and photos of the machining workshop.

Figure 3 shows the annual energy consumption for this machining plant in 2018. The overall annual energy consumption was 2.63×10^7 kWh, and manufacturing processes (machining and heat treatment) consumed about 58% of the total energy. The auxiliary section of the chart represents the energy used for building operation, such as the HVAC system and lighting. Chillers and fans accounted for most of the energy use in this sector, and they consumed 1.41×10^6 kWh and 1.44×10^6 kWh of electricity, respectively. The chillers and fans were components of a complex ventilation system designed to maintain thermal comfort and indoor air quality. In this study, we refer to the current ventilation system in the plant as the "existing ventilation system."

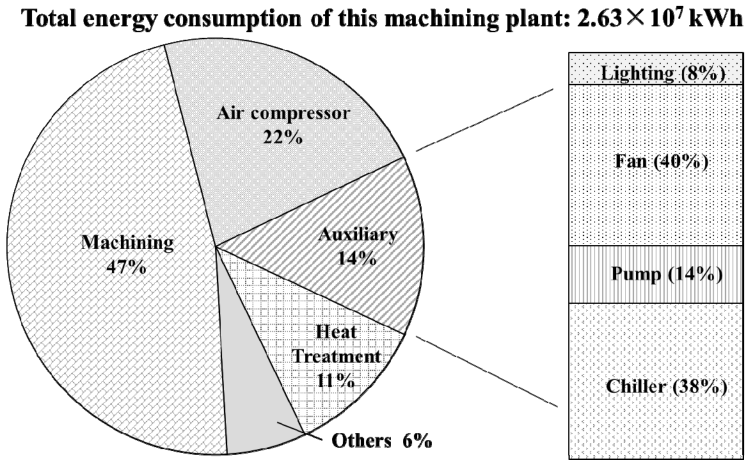

Figure 3. Annual energy consumption by the machining workshop

Figure 4 provides a schematic diagram of the existing ventilation system in the machining plant. Existing ventilation system was consisted of recirculation system, fresh air system and exhaust air system. Recirculation system which was suspended at a height of 4.5 m above the floor had two types of air ducts and air handling units (AHUs) were used in the recirculation system throughout the plant for ventilation and air conditioning. Two make-up air units (MAUs) were employed in the fresh air system which were attached to wall to provide fresh air in summer. Meanwhile, the exhaust fans installed in the roof were sources of significant infiltration.

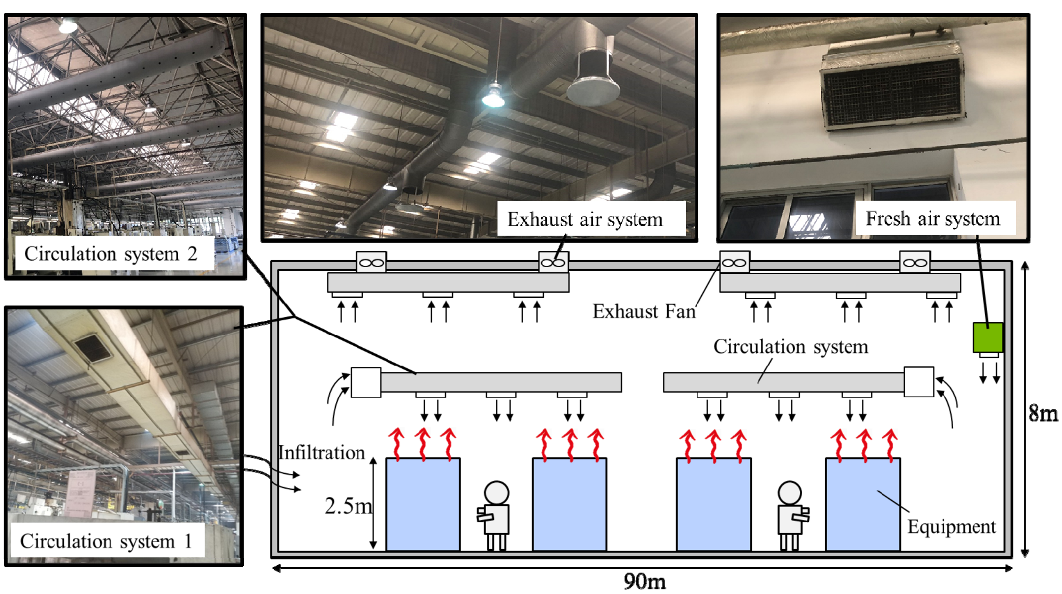

Figure 4. Schematic diagram of the existing ventilation system

To measure indoor air temperature for energy simulation validation, we installed twenty-one air temperature loggers in the middle of the machining plant, as shown in Figure 2. The indoor air temperature was recorded continuously for one week during the cooling season, from September 11 to September 17, 2018, and for another week during the heating season, from November 26 to December 2, 2018. In addition to indoor air temperature, the monthly electricity consumption levels for the chillers, chiller water pumps, and fans in 2018 were obtained for the validation. Meanwhile, surface temperatures, supply air temperature, outdoor air temperature, and particle emission rate were recorded to provide boundary conditions for the CFD simulation.

Heat gains from equipment were an important input to the energy simulation of industrial buildings. This study divided the heat into radiative and convective portions according to our field measurements. Table 1 shows the type and accuracy of measuring equipment. Nearby air temperature and average surface temperature of machining equipment and furnace were measured by multi-parameter ventilation meter and infrared camera respectively. Then radiant and convective heat gains from machining equipment and furnace could be estimated and ratios of radiant heat could be calculated. The calculated ratios of radiant heat from the machining equipment and furnace were 0.5 and 0.8, respectively. The internal heat gains from equipment and lighting were estimated by dividing the annual electricity consumption by the number of working hours. The calculation method of other heat gains such as heat gains from building surfaces, solar heat gains through fenestrations and heat gain due to infiltration were ordinary and they were calculated in EnergyPlus. Supply and exhaust ventilation rates were determined from the ventilation volume recorded in the field measurements. Table 2 provides detailed information about the machining plant and the existing ventilation system, which were used in CFD and BES simulations. This study also obtained local weather data for 2018 from a station located 2 km away from the machining plant. The weather data was used in the building energy simulation.

Table 1. Specifications of measuring equipment

Parameter	Equipment	Range	Accuracy
Air temperature	Multi-parameter ventilation meter (TSI-8386)	-10 ~ 60℃	±0.3℃
Wind speed		0 ~ 50m/s	±0.015m/s
Long term monitored air temperature	Air temperature logger (Risym DHT22)	-40 ~ 80℃	±0.5℃
Surface temperature	Infrared camera (VARIOCAM® HD RESEARCH 900)	-40 ~ 2000℃	±1℃

Table 2. Building and ventilation system information for the machining plant

Parameter	Type	Value
Daily work schedule	Four shifts per day	08:00-12:00 13:00-17:00 21:00-01:00 02:00-06:00
Internal heat gain	Machining	2850

(kW)	Furnace	550
	Lighting	50
	People	36
Ventilation volume (m^3/s)	Supply	329.2
	Exhaust	213.0
Surface temperature (winter/summer) (^oC)	Wall	20/33
	Equipment	21/35
	Floor	19/33
	Roof	21/39
Infiltration air temperature (winter/summer) (^oC)	/	-3/35
Supply air temperature (winter/summer) (^oC)	/	32.0/22.3
Particle emission rate (kg/s)	Each piece of equipment	2.8×10^{-7}

2.2 CFD and BES simulations

Based on the information from the field survey, CFD and BES models of the machining workshop were built in the Fluent and EnergyPlus programs. Commercial CFD software ANSYS Fluent [32] was employed by Wei [43] to simulate temperature, air velocity and pollutant conditions of this plant, the vertical air temperature gradient and pollutant distribution of which were then used in EnergyPlus [33] to predict energy consumption. The simulation was first performed on the existing ventilation system under the actual scenario in 2018 to validate the accuracy of the results. After completing the validation, we compared the annual energy consumption for the three ventilation systems under the same levels of pollutant concentration and average air temperature.

To ensure that the energy consumption levels of different ventilation systems were compared at the same pollutant and average air temperature levels, and to account for the varying temperature gradient in the energy simulation, a framework was proposed to indirectly couple CFD with BES, as shown in Figure 5. First, the allowable pollutant concentration and acceptable thermal comfort levels were achieved by finding a suitable supply flow rate and supply air temperature in CFD. Next, the vertical temperature gradient calculated by CFD was adjusted according to the air conditioning load before feeding this information to the BES to predict energy consumption. The following provides a more detailed description.

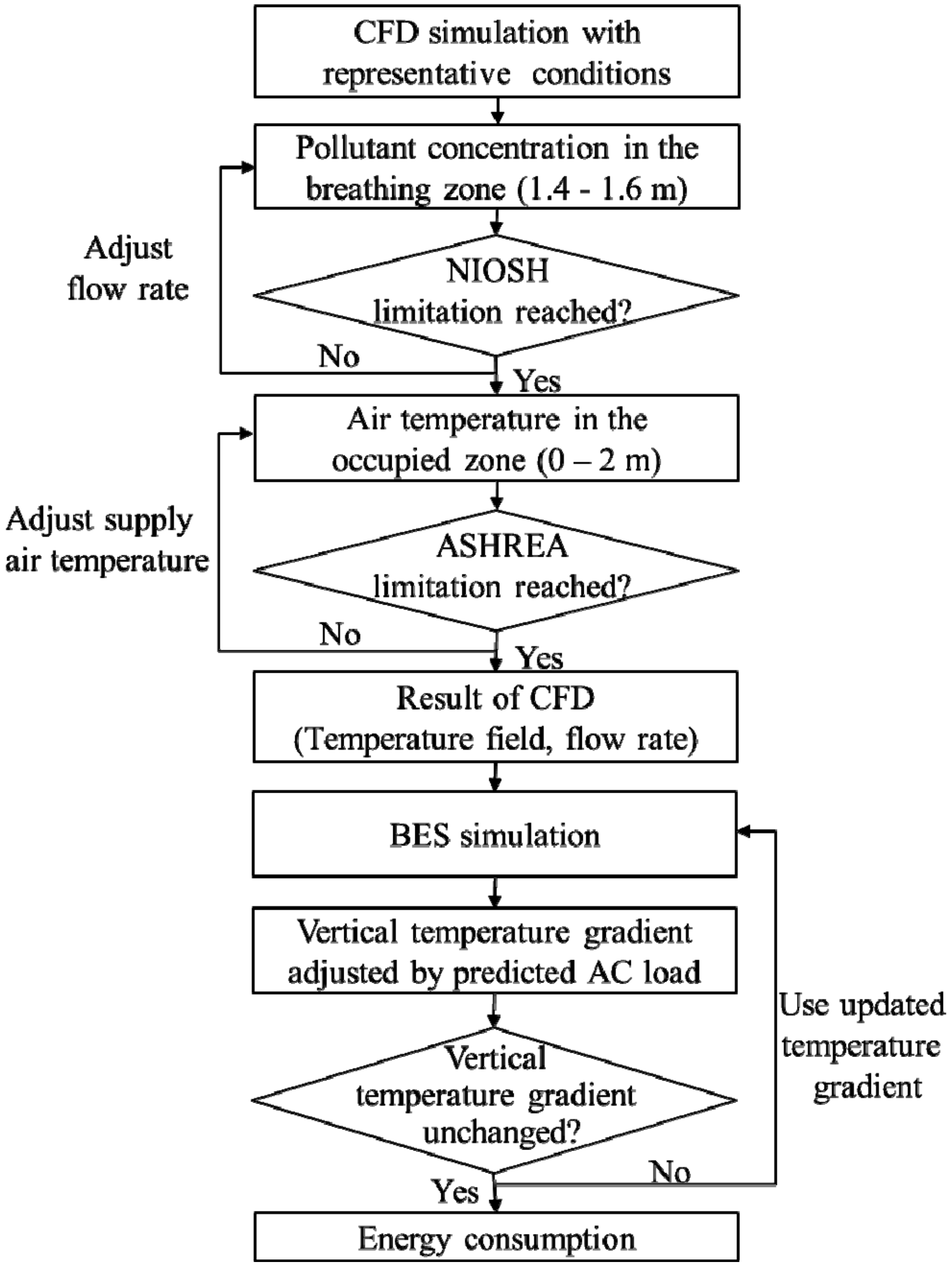

Figure 5. Framework for indirect coupling of CFD and BES for industrial buildings

The first step of the indirect coupling scheme was to find the ventilation rate that could provide the allowable pollutant concentration. Constant-volume ventilation systems are used for industrial buildings because the pollutant emission level of a manufacturing process varies little in the course of a year, and the pollutant field is determined mainly by the ventilation rate [34]. Here, the ventilation rate was found by adjusting the flow rate in the CFD calculation until the pollutant concentration met the standard. In our study, the manufacturing process would generate metalworking fluid aerosols [35], and a particle concentration of 500 ug/m^3 in the breathing zone (1.4 to 1.6 m) was used as the limit, as recommended by the National Institute for Occupational Safety and Health (NIOSH) [36].

The second step was to adjust the supply air temperature in the CFD simulation until the air temperature in the occupied zone (0-2 m) satisfied the thermal comfort requirement for workers. In this study, the summer set point was 25 ºC, while the winter set point was 18 ºC, as recommended by the American Society of Heating. Refrigerating and Air-conditioning Engineers (ASHRAE) [37]. Please note that the supply air temperature determined at this point was used in the CFD simulation only to obtain the temperature gradient; it was not the supply air temperature that was used in the building energy simulation. In the BES, the supply air temperature was determined automatically according to the ventilation rate and air conditioning load.

After the air temperature gradient was obtained by CFD, the third step was to adjust the air temperature gradient by assuming that it was proportional to the air conditioning load. Chen [21] found that such an assumption would not lead to significant error in the energy simulation. As shown in Figure 5, the air temperature gradient was iteratively updated according to AC load until it converged. The iteration was performed with the Energy Management System (EMS) feature in EnergyPlus. When the air temperature gradient was imported to EnergyPlus, the method by Griffith [38] was employed with a non-dimensional height room air model.

Figure 6 shows examples of the change in air temperature gradient for different air conditioning loads with the existing ventilation system in the plant during the cooling season. The air temperature in the occupied zone was constant under different air conditioning loads. The lower the load, the smaller was the temperature difference between the occupied zone and the supply air, return air and indoor average temperature. Under this assumption, we could quickly calculate the annual energy consumption of an industrial building with reasonably good accuracy.

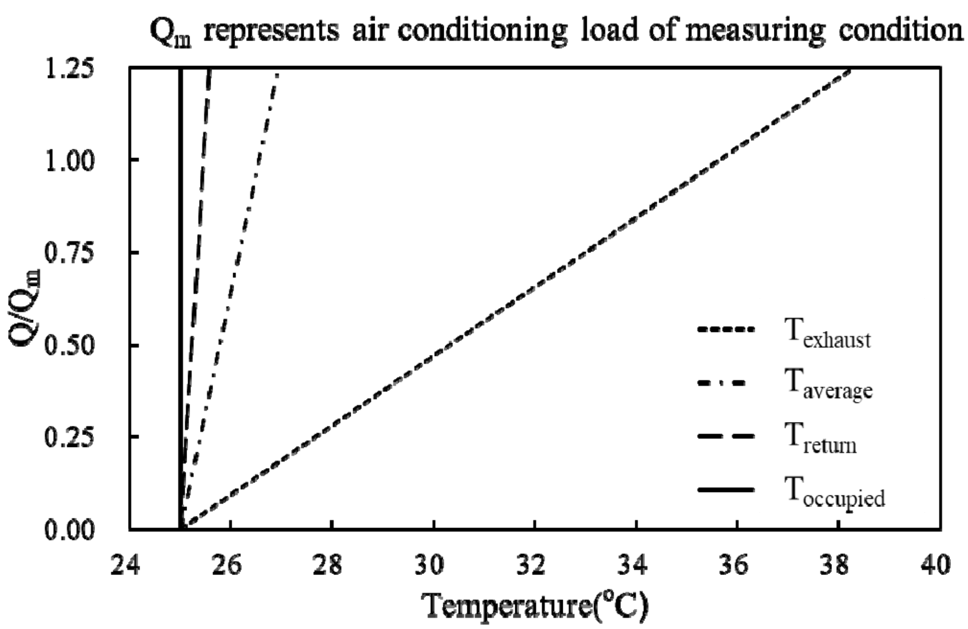

Figure 6. Temperature difference with existing ventilation system for different air conditioning loads

Indirect coupling of CFD and BES was necessary only for a ventilation system that created a temperature gradient. For mixing ventilation, the pollutant concentration and air temperature were assumed to be uniform throughout the entire space.

Therefore, we needed only the ventilation rate, Q (m^3/s), which could be easily calculated by:

$$Q = \frac{\dot{S}}{(C - C_s)} \tag{1}$$

where $\dot{S}$ is the pollutant emission rate (mg/s), C the particle concentrations of indoor air (500 ug/m^3 in this study), and C_s the particle concentration of supply air, which was zero in this study under the assumption of complete removal of particles by a filter.

2.3 Validation of simulations

A large number of uncertain variables can impact the energy consumption of a building [39], and many parameters, such as the heat gain from equipment and the infiltration rate, cannot be accurately obtained through field measurements. Before an energy simulation program can be used to compare the energy use for different ventilation systems, the simulation must be validated to ensure accuracy [40]. This study sought to validate the energy simulation by comparing the measured and predicted indoor air temperatures in the machining plant with the use of the existing ventilation system. The energy consumption for the existing system in 2018 was also calculated and compared with the measurement results. Please note that the objective in validating the simulation was to compare the predicted outputs with the measurements under actual conditions [41]. Hence, the ventilation rate and supply air temperature in the validation simulation were not determined by the framework proposed in Figure 5; rather, they were the measured values displayed in Table 2.

Following the recommendation of ASHRAE [42], two indices, the normalized mean bias error (NMBE) and the coefficient of variation of the root-mean-square error (CV(RMSE)), were used to determine whether the simulation accuracy was acceptable. NMBE and CV(RMSE) are defined as follows:

$$NMBE = \frac{\sum(V_{actual} - V_{modeled})}{(N-1) \times Mean(V_{actual})} \times 100\% \tag{2}$$

$$CV(RMSE) = \frac{\sqrt{\frac{\sum(V_{actual} - V_{modeled})^2}{N-1}}}{Mean(V_{actual})} \times 100\% \tag{3}$$

where V_{actual} is the measured value, $V_{modeled}$ the value predicted by the simulation, and N the number of data points. According to ASHRAE, a model can be considered calibrated if NMVE < 5% and CV(RMSE) < 15% when monthly data are used, or NMVE < 10% and CV(RMSE) < 30% when hourly data are used [42].

In addition to the energy simulation, the CFD program was validated with the use of measured air temperature and contaminant concentration in several locations in a high-ceiling lab with heat and pollutant sources. Further information concerning the CFD modeling of this plant can be found in Wei et al. [43].

2.4 Energy simulation of three ventilation systems

The main objective of this study was to compare the annual energy consumption for three ventilation systems (mixing ventilation, existing ventilation and displacement ventilation).

We assumed a perfect mixing system, which was an ideal condition. Clean air was supplied to the plant, and contaminated air was exhausted form the plant. A portion of the exhausted air was recirculated after being cleaned by filters. The distributions of the air temperature and contaminant concentration were assumed to be uniform.

Figure 4 portrays the existing ventilation system in the machining plant. Air handling units (AHUs) were suspended at a height of 4.5 m above the floor, and clean air was supplied through an inlet duct. One portion of the contaminated air was returned to the AHUs, while another portion was exhausted to the outdoors through fans on the roof. To remove particles from the return and exhaust air, filters were installed in the AHUs and exhaust fans. The AHUs blew air downward, while the thermal plumes from the machines rose upward. The opposing airflows may have created numerous large vortexes and reduced ventilation efficiency.

Figure 7 illustrates the displacement ventilation system proposed by Wei [43]. Compared to traditional displacement ventilation system, it has three advantages: (a) supply air outlets were distributed throughout the plants for better interior ventilation; (b) supply air ducts were attached to columns for less space used; and (c) all fresh air mode to reduce energy uses on filtering. Clean air is delivered to the outlet near the floor through columns to dilute the pollutants and cool the air in the occupied zone. Air is then heated by the machining equipment and rises upwards to the exhaust fans in the roof. The single-direction airflow provided by the new displacement ventilation system could improve the heat and pollutant removal efficiency. Therefore, there was no need for auxiliary exhaust air duct. To maintain the airflow pattern of displacement ventilation, the supply air temperature should be lower than the indoor temperature even in winter. Pure fresh air is used by the displacement ventilation system. In winter, cold outdoor air is heated to a slightly lower temperature than that of the indoor air, and an additional infrared heater system installed above the workers is used to ensure thermal comfort in the plant.

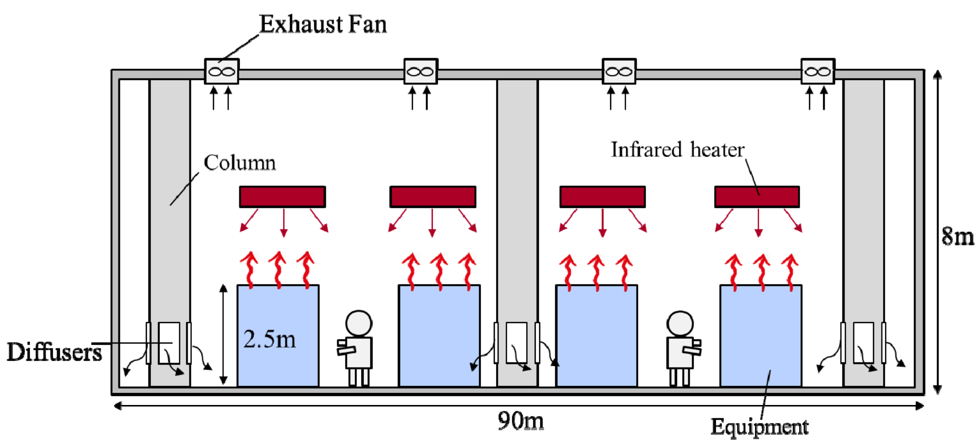

Figure 7. Schematic diagram of the proposed displacement ventilation system

Table 3 lists the parameters of the three ventilation systems. These parameters were used in the BES to ensure that the systems were compared at the same average air temperature and pollutant concentration levels. All three systems used AHUs, and the displacement ventilation system also used infrared heaters in winter. Each AHU used a chiller as the cooling source in the cooling season, and municipal hot water as the heat source. The infrared heaters in the displacement ventilation system employed gas as the heat source. Because of their different pollutant removal efficiencies, the three ventilation systems required different air flow rates. Since displacement ventilation has the highest pollutant removal efficiency, this system required the lowest ventilation flow rate, 347.3m^3/h. The ventilation rates for the mixing ventilation and existing ventilation systems were similar, and they were about twice that for displacement ventilation. Because the displacement ventilation system used outdoor air, its exhaust air volume was equal to the supply air volume. The exhaust air volumes for other two systems were consistent with the actual values recorded in the field survey. Since the displacement ventilation system used outdoor air, which was relatively clean, it needed only a low-efficiency filter with low resistance (110 Pa). The other two systems required high-efficiency filters with high resistance (290 Pa) to clean the polluted return air. Meanwhile, the displacement ventilation system used a shorter duct than the other two systems. With lower filter and duct resistance, the fan head pressure in the displacement ventilation system was lower than in the other two. The capacity of the chiller was determined from the air conditioning load for the design day, to ensure that the set point temperature could be reached year-round. In particular, the infrared heater in the displacement ventilation system was designed by ASHRAE's effective radiant flux method [44] in order to provide the same operating temperature throughout the year.

Table 3. Information about the three ventilation systems

Parameter	Ventilation system		
	Perfect mixing	Existing	Displacement
HVAC equipment	AHU	AHU	AHU+ infrared heater
HVAC operation mode	Return air	Return air	Outdoor air
Supply air volume（m^3/s）	677.9	727.6	347.3
Exhaust air volume（m^3/s）	213	213	347.3
Filter resistance (Pa)	290	290	110
Fan pressure (Pa)	500	500	220
Chilled water Pump (m^3/h)	1166	1080	1181
Hot water Pump (m^3/h)	345	366	607
Chiller (kW)	4594	3734	4134

3. Results

3.1 Validation of energy simulation for existing ventilation system

Figure 8 shows the predicted and measured indoor air temperatures in a one-week period for the cooling and heating seasons. The outdoor air temperature is also provided. The measured indoor temperature is the mean temperature from the 21 sensors installed in the middle of plant. The average of the temperatures predicted by EnergyPlus for the same zone and height are used in the comparison. According to Figure 8, the trend of the temperature variation in the simulation was similar to that for the measured temperature. The minimum daily indoor temperatures appear from 06:00 to 08:00 and from 20:00 to 21:00, which are different from the time periods with minimum outdoor temperature. This is because a four-shift work schedule was implemented in the plant, and there were breaks from 06:00 to 08:00 and from 20:00

to 21:00. When the heat gains from the machining process became smaller, the temperature would decrease. In summary, there was good agreement between the measured and simulated air temperature.

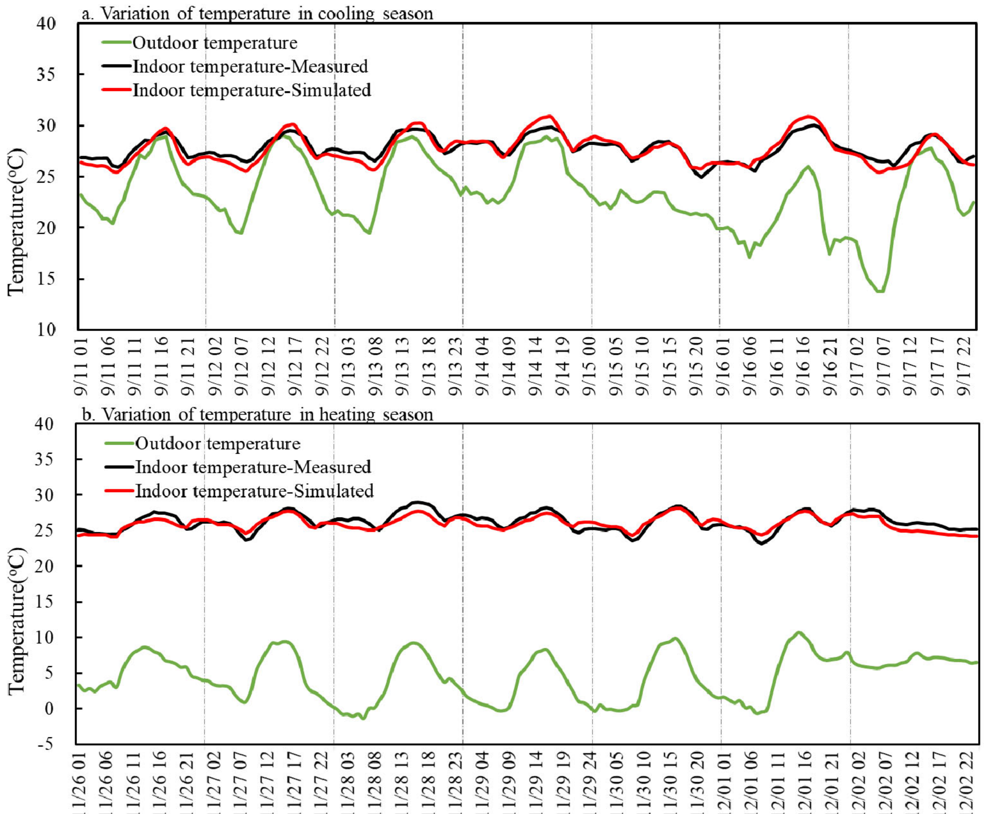

Figure 8. Comparison of simulated and measured air temperature in the machining plant for a one-week period in: (a) the cooling season;(b) the heating season

Figure 9 compares the simulated energy consumption with the actual energy data from the plant, and the agreement between the two is good. The chiller and the chiller pump were in operation from May to September. In particular, the chiller worked for only five days in May, based on the actual conditions recorded in the field measurements. The energy consumption by the fans was high in summer and winter, and low in the transitional seasons. This was because only the exhaust fans were working in the transitional seasons, while the supply air fans operated only when heating/cooling was needed.

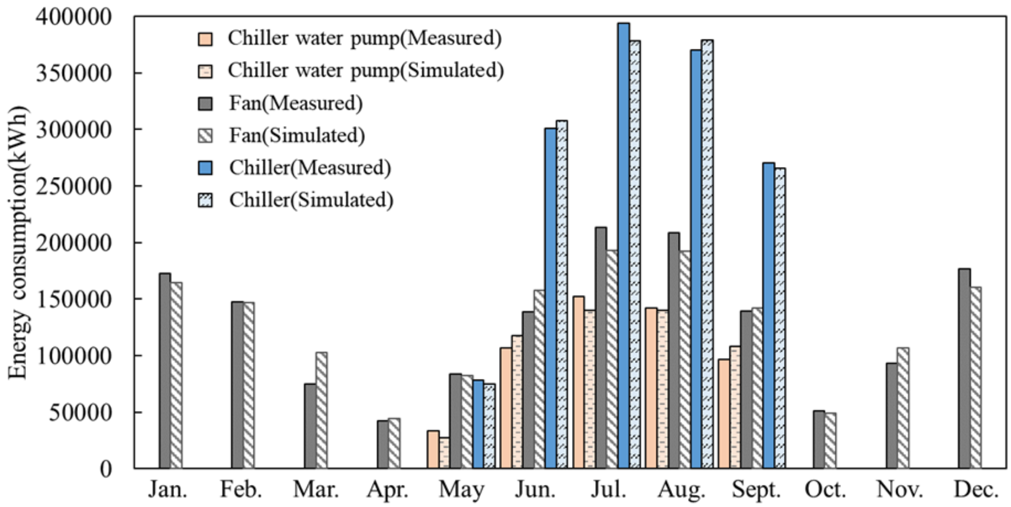

Figure 9. Comparison of energy consumption between the data and the simulation

Table 4 summarizes the NMBE and CV(RMSE) indices for the measured and simulated data shown in Figures 8 and 9. The values of these indices were smaller than the ASHRAE limits [42]. Thus, the simulation was validated, and the energy simulation model was accurate. The model could then be used to predict the energy consumption for the HVAC systems in the machining plant.

Table 4. Error analysis for the energy simulation

Validation parameter	Data frequency	Indices	Index value	ASHRAE limit
Chiller energy consumption	Monthly	NMBE	0.77%	5%
		CV(RMSE)	3.62%	15%
Fan energy consumption	Monthly	NMBE	-0.03%	5%
		CV(RMSE)	11.30%	15%
Pump energy consumption	Monthly	NMBE	-0.45%	5%
		CV(RMSE)	9.80%	15%
Temperature of cooling season	Hourly	NMBE	0.38%	10%
		CV(RMSE)	2.05%	30%
Temperature of cooling season	Hourly	NMBE	0.15%	10%
		CV(RMSE)	0.47%	30%

3.2 Comparison of the three ventilation systems

Next, this study used the validated EnergyPlus software to compare energy consumption by the mixing, existing, and displacement ventilation systems according to the method described in Section 2.2. The first step was CFD calculation of the pollutant and temperature gradients in the plant with the three different systems.

3.2.1 Vertical pollutant and temperature gradients for the three ventilation systems

Figure 10 displays the vertical particle concentration gradient for the three ventilation systems in the cooling and heating seasons. Particle concentration was assumed to be uniform for the perfect mixing ventilation system. Flow rate of three ventilation systems were determined while average pollutant concentration of the breathing zone (1.4-1.6 m) were equal to 500 ug/m^3. The existing ventilation system created a uniform pollutant field in the lower part of the plant, and a negative pollutant concentration gradient in the upper part. This occurred because the supply air outlets were positioned 4.5 m above the ground; the jet flow and thermal plume moved in opposite directions; and large vortexes trapped pollutants in the lower part of the plant. It was difficult for the exhaust fans in the ceiling to remove pollutants from the lower part. To solve those problem, the displacement ventilation system with lower supply air velocity created unidirectional airflow. It drew the pollutants from the occupied zone toward the ceiling and discharged them through the exhaust fans, thus improving the pollutant removal efficiency. Because it had the highest efficiency, the displacement ventilation system required the lowest ventilation flow rate and its lower supply air velocity would avoid draught in the occupied zone.

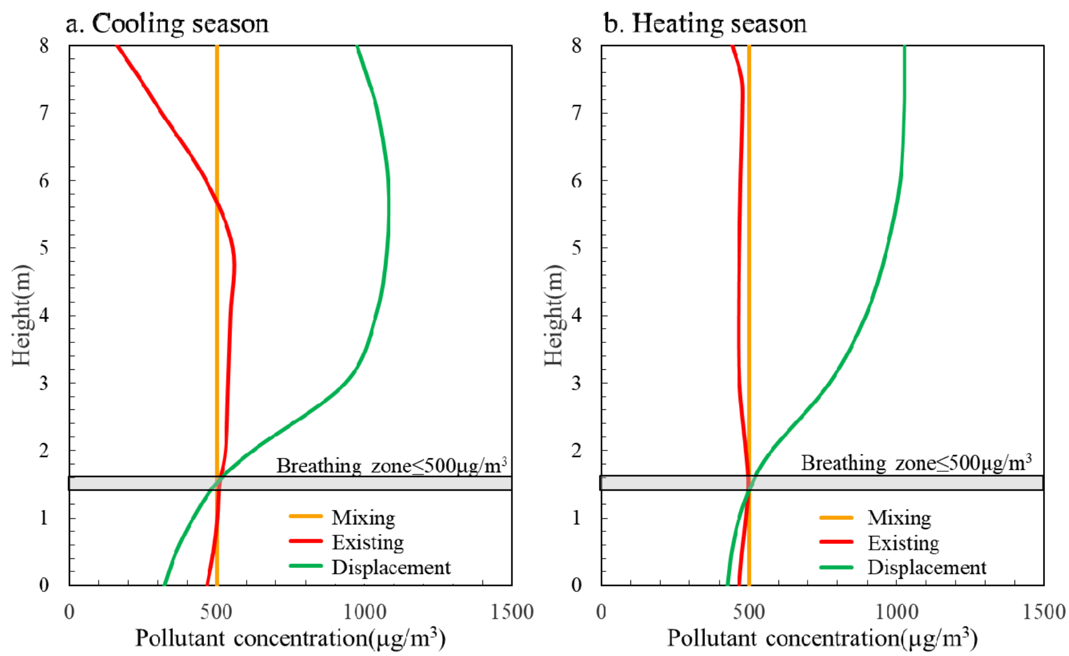

Figure 10. Vertical pollutant concentration gradient for the three ventilation systems: (a) in the cooling season;(b) in the heating season

Figure 11 shows the vertical temperature gradient for the three ventilation systems in the cooling and heating seasons. The mixing ventilation system was assumed to provide uniform air temperature. The temperature variation in the occupied zone was very small for the existing ventilation system in both summer and winter. A larger vertical temperature gradient existed with displacement ventilation, but the vertical temperature difference between head level (1.7 m) and ankle level (0.1 m) was 2.1 K which was under the 3 K limitation of ASHRAE [37]. Using average air temperature of the occupied zones to represent thermal comfort was acceptable and can be conveniently used to control air-conditioning systems. Therefore, the supply air temperature of three ventilation systems were determined with the same average air temperature of the occupied zone (0-2 m). In the cooling season, the mean air temperature in the occupied zone was satisfactory. In the heating season, in order to save energy, the temperature to which the supply air was heated was lower than the air temperature in the plant. This was done to maintain the flow characteristics of displacement ventilation. As a result, the mean air temperature in the occupied zone was only 16°C, which was lower than the design temperature of 18°C. To maintain an acceptable thermal comfort level, infrared heaters were used to provide overhead heating.

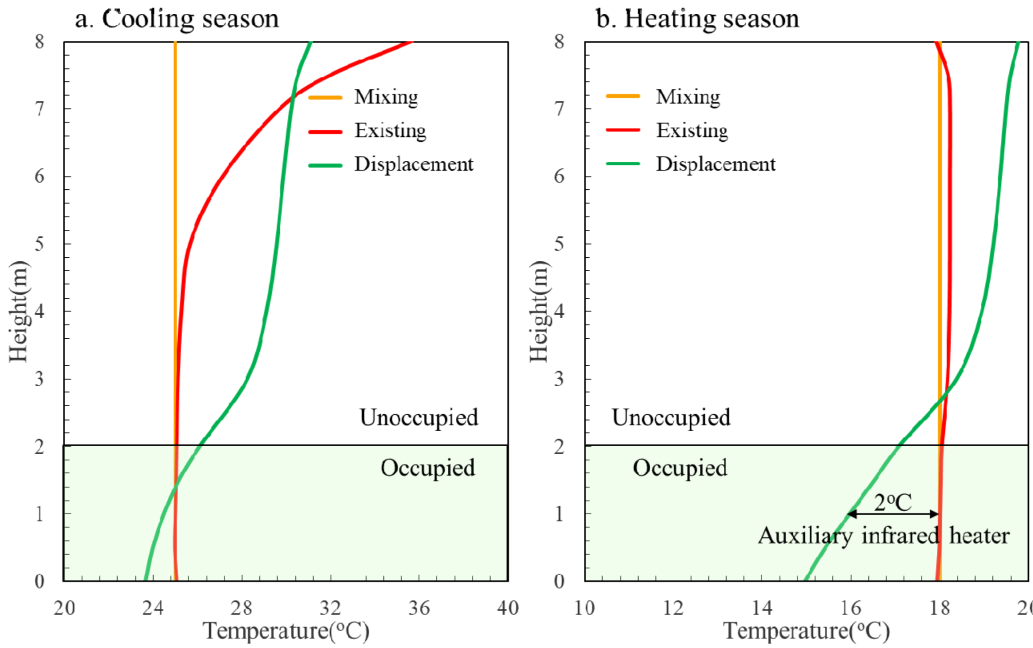

Figure 11. Vertical temperature gradient with three different ventilation systems: (a) in the cooling season;(b) in the heating season

3.2.2 Energy analysis for the three ventilation systems

Figure 12 displays the total annual energy consumption in terms of electricity, municipal hot water and gas, in units of kWh. The displacement ventilation system had the lowest fan head pressure and lowest ventilation flow rate. As a result, the fan energy consumption for this ventilation system was 53.9% lower than for the existing system and 59.7% lower than for mixing ventilation. Compared to perfect mixing, the existing ventilation system had a lower ventilation efficiency and consumed 14.4% more energy for fan operation. The chillers in the displacement and existing ventilation systems consumed 9.5% and 3.9% less electricity, respectively, than the chiller in the mixing ventilation system. This difference arose because the former two systems delivered cooled air to the occupied zone more effectively than the mixing ventilation. Compared to the fan and chiller, the pump had low electricity consumption. Displacement ventilation system had the lowest cooling energy consumption and highest heating energy consumption. As a result, its electricity consumption of the pump in displacement ventilation was greater than that for the existing ventilation system and less than that for mixing ventilation.

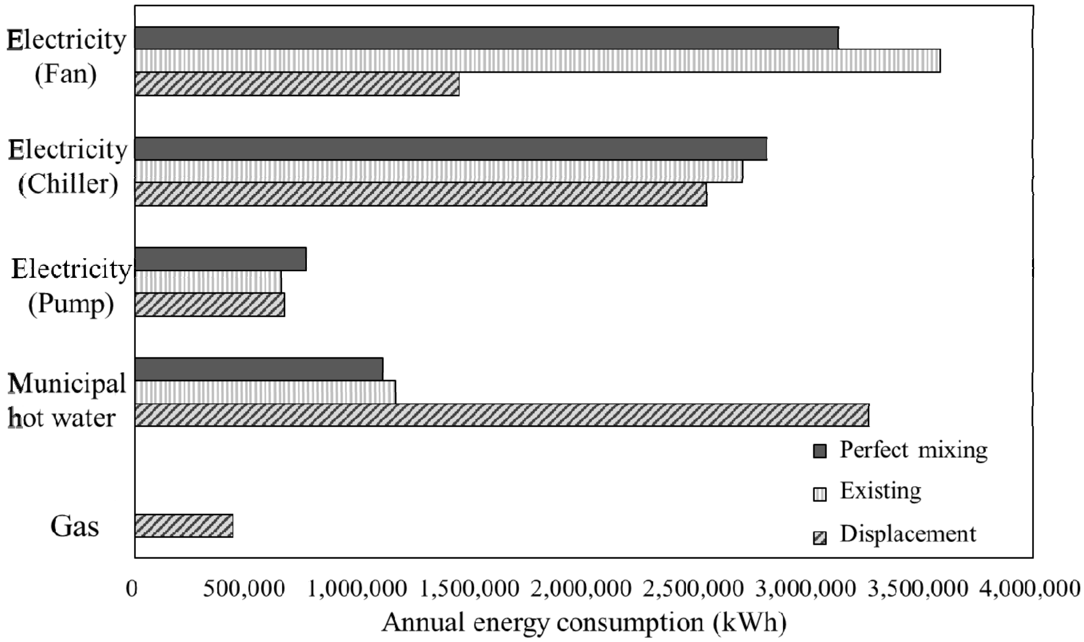

Figure 12. Different types of energy consumption for the three ventilation systems

The displacement ventilation system consumed considerably more municipal hot water than the mixing and existing ventilation systems did. This was because the displacement ventilation had to heat 347.3 m^3/h of cold outdoor air to room temperature, whereas the other two systems only needed to heat infiltration air, which was equal to the exhaust air volume of 213 m^3/h. In addition, the displacement ventilation system used gas as fuel for the infrared heaters to maintain thermal comfort. In total, displacement ventilation consumed three times as much energy for heating as did the other two systems. The consumption levels of municipal hot water were similar for the existing and mixing ventilation systems.

To compare the operating costs for the three ventilation systems, energy consumption levels were transformed to costs. The AHUs used municipal hot water for heating at a cost of 0.7343 Yuan/kWh; the radiant panels used gas for heating at 0.216 Yuan/kWh; and other equipment such as the chillers, pumps, and fans consumed electricity at 0.31 Yuan/kWh. Figure 13 shows the monthly energy costs for the three different ventilation systems. While heating energy costs varied considerably, energy costs for the chillers did not differ greatly across the cooling months. This was because the heating load was influenced mainly by outdoor weather conditions, whereas the cooling load was affected by a combination of outdoor weather conditions and by the internal heat gains from the equipment.

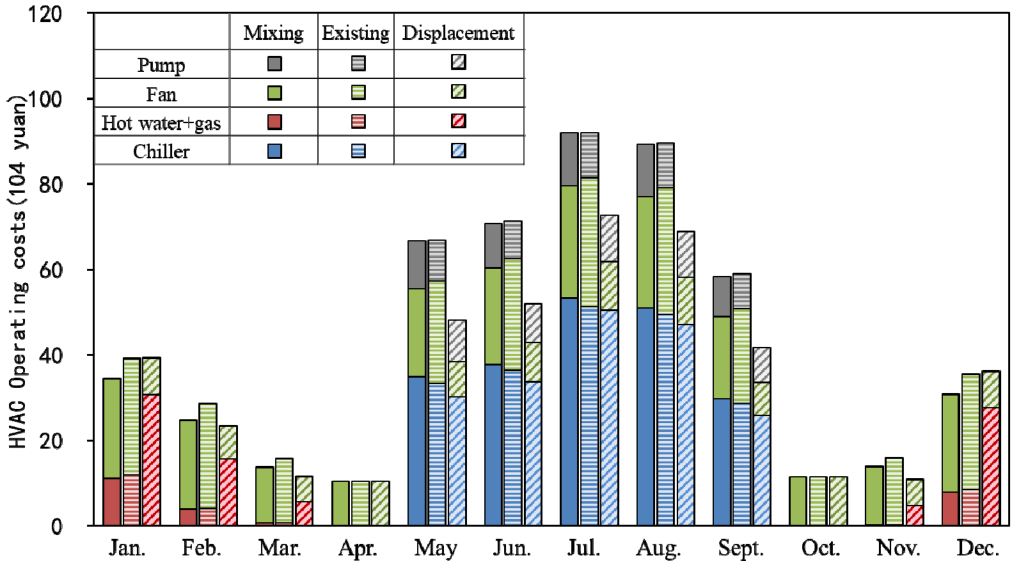

Figure 13. Monthly energy costs for the chiller, hot water plus gas, and fan for the three ventilation systems

Based on actual HVAC system operation in this plant, only exhaust fans were operating and consuming energy in April and October. Compared to mixing ventilation, the existing ventilation system used less energy for cooling and more energy for heating. Because pollutants were trapped in the lower part of the plant, the existing ventilation system needed a higher ventilation rate and thus more energy for fan operation. The total annual energy cost for the existing ventilation system was higher than that for mixing ventilation. Displacement ventilation with the all-fresh-air mode had both advantages and disadvantages. On one hand, displacement ventilation consumed a large amount of energy to heat fresh air in winter. On the other hand, it did not require a high-efficiency filter to clean the polluted return air. Thus, the energy cost for fan operation was reduced. Because of the lower energy cost ratio for municipal hot water and gas than for electricity, the energy saving for fan operation exceeded the heating energy increase. Compared to the costs for mixing and existing ventilation, the total annual energy cost for displacement ventilation was reduced by 17.5 % and 20.3%, respectively.

4. Discussion

4.1 Comparing simulation speed and accuracy for different methods

This study proposed a framework for indirect coupling of CFD and BES for the prediction of energy consumption in large industrial buildings. Simulating one case in CFD required more than 10 hours, and it would have been too expensive to perform repeated simulations for different conditions with varying outdoor climate. Therefore, the assumption that a vertical room air temperature gradient is proportional to the air conditioning load was employed in this study. Although the assumption may cause a discrepancy in energy consumption predictions, it still provides much higher accuracy than other approaches such as assuming a uniform air temperature or a fixed air temperature difference [21]. Table 5 summaries simulation speed and accuracy of different simulation methods. The new framework had a good balance between speed and accuracy. By providing temperature gradient, the proposed indirect coupling framework had a better accuracy than mixing model and zonal model. At the same time, the proposed indirect scheme reduced computational time compared with direct coupling scheme. Compared with existing indirect coupling method, this proposed method can consider various outdoor climate conditions by updating air temperature gradient with air conditioning load.

Table 5. Speed and accuracy of different simulation methods

Model		Computing Time			Simulation ability		
		CFD[a]	BES[a]	Speed	Pollutant distribution	Temperature gradient	Varied conditions
Mixing model		/	3*2min	Good	Bad	Bad	Bad
Zonal model		/	3*2min	Good	Bad	Normal[b]	Normal[c]
Indirect coupling CFD and BES	Past research[27-31]	3*2*10h	3*2min	Normal	Good	Good	Bad
	New framework	**3*2*10h**	**3*2min**	**Normal**	**Good**	**Good**	**Normal**[c]
Coupling CFD and BES		3*8760*10h	/	Bad	Good	Good	Good

a. '3' means three ventilation system; '2' or '8760' mean two typical case or 8760 case for all year; '10' or '2' means each case would consume about 10 h for CFD and 2 min for BES.

b. Zonal model could consider temperature gradient, but it could not accurately predict temperature gradient in industrial buildings

c. The proposed scheme could consider the effect of outdoor climate on temperature gradient by updating the gradient with air conditioning load

4.2 Assumptions and limitations

Internal heat gains from equipment were difficult to measure, but they had a significant impact on the air conditioning load. Under the assumption that equipment heat gains remained the same over time, we calculated the size of the gains according to the equipment energy usage and operating schedule.

Thermal comfort is influenced by many environmental parameters such as air temperature, air velocity, radiant temperature, and humidity [45][46]. In this study, we only considered average air temperature of the occupied zones for thermal comfort, and used the air temperature to control ventilation system.

The energy consumption for the three ventilation systems was compared at the same pollutant and thermal comfort levels by using the indirect coupling framework. The simulations were intended to be consistent with practical operation strategy. The ventilation system stopped working when the air conditioning load was zero and only exhaust air system kept working to eliminate contaminated air. Although thermal comfort and air quality could not be fully guaranteed, the comparison of energy consumption under such a strategy nevertheless revealed the advantages and disadvantages of the three ventilation systems.

5. Conclusions

This paper proposed an improved displacement ventilation system for a machining plant in Tianjin, China, and compared the system's energy consumption with that for mixing and existing ventilation systems. The energy consumption for the three systems was simulated by coupling CFD and BES. The temperature gradient obtained by CFD was proportionally adjusted according to the air conditioning load. The energy consumption by different ventilation systems was compared at the same pollutant and thermal comfort levels. The research method was validated by comparing the predicted and measured indoor air temperature and energy consumption of the machining plant. The investigation led to the following conclusions:

- The energy consumption by fans in the displacement ventilation system was less that for existing and mixing ventilation by 53.9% and 59.7%, respectively. This difference was due mainly to the high pollutant removal efficiency and low required ventilation rate of displacement ventilation. In addition, the filter resistance in the displacement ventilation system was low because the system did not require a high-efficiency filter to clean the polluted indoor air. The total energy cost for displacement ventilation was 20.3% lower than that for the existing ventilation system and 17.5% lower than that for mixing ventilation.
- The displacement ventilation system was effective in supplying cool air to the occupied zone, so that the energy use in the cooling season was lower than that for the other two systems. However, because of the need to heat a large amount of outdoor fresh air to the room air temperature, displacement ventilation was not efficient in the heating season, and it consumed more heating energy in the winter. A heat exchanger should be used in displacement ventilation to save energy for heating.
- Both vertical temperature stratification and pollutant removal efficiency had a significant impact on energy consumption by the ventilation systems. The new framework accounts for these factors by coupling CFD and BES, and is therefore recommended for predicting annual energy consumption in industrial buildings in the future.

ACKNOWLEDGEMENT

This study was supported by the National Key R&D Program of the Ministry of Science and Technology, China, on "Green Buildings and Building Industrialization" through Grant 2018YFC0705300.

REFERENCES

[1] National Bureau of Statistics of the People's Republic of China, China Energy Statistical Yearbook, Beijing: China Statistics Press, 2018.
[2] Y. Wang, Y. Cao, X. Meng, Energy efficiency of industrial buildings, Indoor Built Environ. 28 (2019) 293–297.
[3] G. Gourlis, I. Kovacic, A study on building performance analysis for energy retrofit of existing industrial facilities, Appl. Energy. 184 (2016) 1389–1399.
[4] H. Wan, Y. Li, W. Yang, Analysis on the state, composition, and characteristics of industrial building energy consumption in Dongguan, Building Energy Efficiency 33 (1) (2007) 230–231 (In Chinese).
[5] A.C. Caputo, P.M. Pelagagge, Upgrading mixed ventilation systems in industrial conditioning, Appl. Therm. Eng. 29 (2009) 3204–3211.
[6] J. Lau, Q. Chen, Energy analysis for workshops with floor-supply displacement ventilation under the U.S. climates, Energy Build. 38 (2006) 1212–1219.
[7] E. Division, Analysis of energy use in building services of the industrial sector in California: Two case studies, Energy Build. 19 (1992) 133–141.
[8] D. Katunsky, A. Korjenic, J. Katunska, M. Lopusniak, S. Korjenic, S. Doroudiani, Analysis of thermal energy demand and saving in industrial buildings: A case study in Slovakia, Build. Environ. 67 (2013) 138–146.
[9] K. Ahmed, E. Sistonen, R. Simson, J. Kurnitski, J. Kesti, P. Lautso, Radiant panel and air heating performance in large industrial buildings, Build. Simul. 11 (2018) 293–303.
[10] L. Tian, Z. Lin, Q. Wang, Experimental investigation of thermal and ventilation performances of stratum ventilation, Build. Environ. 46 (2011) 1309–1320.
[11] Z. Lin, C.K. Lee, S. Fong, T.T. Chow, T. Yao, A.L.S. Chan, Comparison of annual energy performances with different ventilation methods for cooling, Energy Build. 43 (2011) 130–136.
[12] K. Lee, T. Zhang, Z. Jiang, Q. Chen, Comparison of airflow and contaminant distributions in rooms with traditional displacement ventilation and under-floor air distribution systems, ASHRAE Trans. 115 PART 2 (2009) 306–321.
[13] H. Qian, Y. Li, P. V. Nielsen, C.E. Hyldgaard, T.W. Wong, A.T.Y. Chwang, Dispersion of exhaled droplet nuclei in a two-bed hospital ward with three different ventilation systems, Indoor Air. 16 (2006) 111–128.
[14] G. Cao, H. Awbi, R. Yao, Y. Fan, K. Sirén, R. Kosonen, J. (Jensen) Zhang, A review of the performance of different ventilation and airflow distribution systems in buildings, Build. Environ. 73 (2014) 171–186.
[15] H.X. Zhao, F. Magoulès, A review on the prediction of building energy consumption, Renew. Sustain. Energy Rev. 16 (2012) 3586–3592.
[16] D. Coakley, P. Raftery, M. Keane, A review of methods to match building energy simulation models to measured data, Renew. Sustain. Energy Rev. 37 (2014) 123–141.

[17] N.M. Mateus, G. Carrilho da Graça, Simulated and measured performance of displacement ventilation systems in large rooms, Build. Environ. 114 (2017) 470–482.
[18] A.C. Megri, F. Haghighat, Zonal modeling for simulating indoor environment of buildings: Review, recent developments, and applications, HVAC R Res. 13 (2007) 887–905.
[19] Y. Yu, A.C. Megri, S. Jiang, A review of the development of airflow models used in building load calculation and energy simulation, Build. Simul. 12 (2019) 347–363.
[20] W. Tian, X. Han, W. Zuo, M.D. Sohn, Building energy simulation coupled with CFD for indoor environment: A critical review and recent applications, Energy Build. 165 (2018) 184–199.
[21] Q. Chen, Indoor airflow, air quality and energy consumption of buildings, Ph.D. thesis, Delft University of Technology, Delft, 1988.
[22] C.O.R. Negrao, Conflation of computational fluid dynamics and building thermal simulation, Ph.D. thesis, University of Strathclyde, Glasgow, UK, 1995.
[23] Z. Zhai, Q. Chen, P. Haves, J.H. Klems, On approaches to couple energy simulation and computational fluid dynamics programs, Build. Environ. 37 (2002) 857–864.
[24] Z. Zhai, Q. Chen, Solution characters of iterative coupling between energy simulation and CFD programs, Energy Build. 35 (2003) 493–505.
[25] J. Srebric, Q. Chen, L.R. Glicksman, Coupled airflow and energy simulation program for indoor thermal environmental studies, ASHRAE Trans. 106 (2000) 465–476.
[26] A. Malkawi, B. Yan, Y. Chen, Z. Tong, Predicting thermal and energy performance of mixed-mode ventilation using an integrated simulation approach, Build. Simul. 9 (2016) 335–346.
[27] C. Liang, X. Li, X. Shao, B. Li, Numerical analysis of the methods for reducing the energy use of air-conditioning systems in non-uniform indoor environments, Build. Environ. 167 (2020).
[28] H. Xu, J. Niu, Numerical procedure for predicting annual energy consumption of the under-floor air distribution system, Energy Build. 38 (2006) 641–647.
[29] Y. Wang, K.K.L. Wong, H. Du, J. Qing, J. Tu, Design configuration for a higher efficiency air conditioning system in large space building, Energy Build. 72 (2014) 167–176.
[30] Y. Cheng, J. Niu, N. Gao, Stratified air distribution systems in a large lecture theatre: A numerical method to optimize thermal comfort and maximize energy saving, Energy Build. 55 (2012) 515–525.
[31] W. Zhang, K. Hiyama, S. Kato, Y. Ishida, Building energy simulation considering spatial temperature distribution for nonuniform indoor environment, Build. Environ. 63 (2013) 89–96.
[32] Ansys Inc. Ansys Fluent User's Guide. Ansys Inc., Canonsburg, Pennsylvania, USA (2012).

[33] U.S. Department of Energy (DOE). EnergyPlus Engineering Reference (Version 9.1.0 Documentation; Building Technologies Program); U.S. Department of Energy: Washington, DC, USA, 2017.
[34] H.Q. Wang, C.H. Huang, D. Liu, F.Y. Zhao, H.B. Sun, F.F. Wang, C. Li, G.X. Kou, M.Q. Ye, Fume transports in a high rise industrial welding hall with displacement ventilation system and individual ventilation units, Build. Environ. 52 (2012) 119–128.
[35] G.M. Piacitelli, W.K. Sieber, D.M. O'Brien, R.T. Hughes, R.A. Glaser, J.D. Catalano, Metalworking fluid exposures in small machine shops: An overview, Am. Ind. Hyg. Assoc. J. 62 (2001) 356–370.
[36] National Institute for Occupational Safety and Health (NIOSH), Criteria for a Recommended Standard: Occupational Exposure to Metalworking Fluids (DHHS [NIOSH] Pub. no. 98–102). Cincinnati, Ohio: NIOSH, 1998.
[37] ANSI/ASHRAE 55-2013, Thermal Environmental Conditions for Human Occupancy, American Society of Heating. Refrigerating and Air-conditioning Engineers Inc., 2013.
[38] B. Griffith, Q. Chen, Framework for coupling room air models to calculations (RP-1222), ASHRAE Trans. (2004) 91–112.
[39] M. Royapoor, T. Roskilly, Building model calibration using energy and environmental data, Energy Build. 94 (2015) 109–120.
[40] S.Ø. Jensen, Validation of building energy simulation programs: a methodology, Energy Build. 22 (1995) 133–144.
[41] T. Salsbury, R. Diamond, Performance validation and energy analysis of HVAC systems using simulation, Energy Build. 32 (2000) 5–17.
[42] ASHRAE Guideline 14, Measurement of Energy and Demand Savings, ASHRAE Standards Committee, 2014.
[43] G. Wei, B. Chen, D. Lai, Q. Chen, An improved displacement ventilation system for a machining plant, Atmos. Environ. (2020) 117419.
[44] ASHRAE Handbook, ASHRAE Handbook–HVAC Applications, American Society of Heating, Refrigerating and Air-Conditioning Engineers, Inc., Atlanta, GA, 2015.
[45] He Manchen, Lian Zhiwei , Chen Pin , Evaluation on the performance of quilts based on young people's sleep quality and thermal comfort in winter, Energy and Buildings 183 (2019) 174–183.
[46] Xia Lulu, Lan Li, Tang Jieyu, Lin Yanbing, Wang Zhengtao, Bed heating improves the sleep quality and health of the elderly who adapted to no heating in a cold environment, Energy and Buildings 210 (2020).